Molecular mechanism of the sweet taste enhancers

Feng Zhang[a], Boris Klebansky[b], Richard M. Fine[b], Haitian Liu[a], Hong Xu[a], Guy Servant[a], Mark Zoller[a], Catherine Tachdjian[a], and Xiaodong Li[a,1]

[a]Senomyx, Inc., San Diego, CA 92121; and [b]BioPredict, Inc., Oradell, NJ 07649

Edited* by Solomon Snyder, Johns Hopkins University School of Medicine, Baltimore, MD, and approved January 25, 2010 (received for review October 12, 2009)

Positive allosteric modulators of the human sweet taste receptor have been developed as a new way of reducing dietary sugar intake. Besides their potential health benefit, the sweet taste enhancers are also valuable tool molecules to study the general mechanism of positive allosteric modulations of T1R taste receptors. Using chimeric receptors, mutagenesis, and molecular modeling, we reveal how these sweet enhancers work at the molecular level. Our data argue that the sweet enhancers follow a similar mechanism as the natural umami taste enhancer molecules. Whereas the sweeteners bind to the hinge region and induce the closure of the Venus flytrap domain of T1R2, the enhancers bind close to the opening and further stabilize the closed and active conformation of the receptor.

positive allosteric modulators | sweet taste receptor | T1R

Humans can detect at least five basic taste qualities, including sweet, umami, bitter, salty, and sour. The sweet and umami taste are mediated by closely related G protein-coupled receptors (GPCRs). The three members of the T1R family form two heteromeric taste receptors: umami (T1R1/T1R3) (1, 2) and sweet (T1R2/T1R3) (1, 3). T1R receptors belong to the class C GPCRs, along with metabotropic glutamate receptors (mGluRs), γ-aminobutyric acid receptor B ($GABA_BR$), calcium sensing receptors (CaSR), and others. The defining motif in these receptors is an extracellular Venus flytrap (VFT) domain (4), which consists of two globular subdomains connected by a three-stranded flexible hinge. The VFT domain contains the orthosteric ligand binding site. The crystal structures of mGluR VFT domains (5, 6) revealed that the bilobed architecture can form an "open" or "closed" conformation. Glutamate binding stabilizes both the "closed" and the "active" dimer conformation. This scheme in the initial receptor activation has been applied generally to other class C GPCRs.

Over the years, researchers have been developing noncaloric sweeteners to reduce dietary sugar intake. Unfortunately, all existing noncaloric sweeteners are characterized by their off taste (7, 8) and fail to mimic the real sugar taste. Since the identification of the sweet taste receptor, a new approach became available, which is to develop positive allosteric modulators (PAMs) of the receptor. These molecules work as sweet taste "enhancers," which possess no taste of their own but potentiate the sweet taste of sugars. Examples of taste enhancers can be found in umami taste, which is known for its unique characteristic of synergism (9). Purinic ribonucleotides such as inosine-5′-monophosphate (IMP) and guanosine-5′-monophosphate (GMP) can strongly potentiate the umami taste intensity of glutamate and are rare examples of naturally occurring GPCR PAMs. In taste tests, 200 μM IMP, which does not elicit any umami taste by itself, can increase human umami taste sensitivity to glutamate by 15-fold (1). We recently illustrated the molecular mechanism of IMP/GMP (10). Our data indicate that glutamate binds close to the hinge region of the VFT domain and induces the closure of the two lobes, whereas IMP and GMP bind near the opening of the domain and further stabilize the closed conformation by coordinating the positively charged residues via their phosphate group.

Allosteric modulators are attracting more and more interest from the pharmaceutical industry as drug candidates. Multiple PAMs (11) for members of class C GPCRs have been identified by screening synthetic chemical libraries. In contrast to IMP and GMP, they all bind to the transmembrane domain and their activities are relatively weak. PAMs have been identified recently for the human sweet taste receptor (Servant et al.). SE-2 is a selective enhancer for sucralose, whereas SE-3 enhances the sweet taste of both sucralose and sucrose. Here we take the chimeric receptor, mutagenesis, and molecular modeling approaches, and propose a molecular mechanism for the enhancement activity of two structurally related sweet taste enhancers.

Results and Discussion

Functional Mapping of Sweet Enhancer Interaction Sites. To understand the mechanism of these sweet taste enhancers, it is important to determine where these molecules bind to the receptor. To identify the functional domain required for interaction with enhancer molecules, we used sweet–umami (10) and human–rat chimeric T1R receptors (12) to map the binding site. The sweet taste receptor and the umami taste receptor share a common subunit, T1R3. Because the sweet taste enhancers have no effect on the umami taste receptor, they most likely bind to the T1R2 subunit, either at the N-terminal extracellular domain (NED; composed of the VFT domain and a small Cys-rich region) or the transmembrane domain (TMD).

We swapped the NED of the sweet and umami receptors to generate sweet–umami chimeras. T1R2-1 consists of the T1R2 NED and T1R1 TMD, and T1R1-2 consists of the T1R1 NED and T1R2 TMD. Each hybrid receptor was coexpressed with T1R3 and assayed for enhancement activity of the sweet enhancers (Fig. 1*A*). SE-2 was used to study the mechanism of sucralose enhancement, and SE-3 was used for sucrose. To elevate the hybrid receptor activity to measurable levels, we coexpressed human T1R1-2 with rat T1R3 instead of human T1R3. T1R2-1/T1R3 responded to sucralose and sucrose, and the activities could be enhanced by SE-2 and SE-3, respectively. In contrast, T1R1-2/T1R3 responded to glutamate and the activity was not enhanced by either SE-2 or SE-3. These observations indicate that the NED of T1R2 is critical for interaction with SE-2 and SE-3, whereas the TMD of T1R2 is not required.

SE-2 and SE-3 are selective for human T1R2/T1R3 and have no effect on the rat receptor. This species selectivity can be exploited to map the interaction sites using human–rat chimeric receptors (Fig. 1*B*). Replacing the human T1R2 NED with its rat counterpart gave rise to a chimeric sweet taste receptor that was not responsive to SE-2 or SE-3. Conversely, replacing the rat

Author contributions: B.K., R.M.F., and X.L. designed research; F.Z., B.K., R.M.F., H.L., and H.X. performed research; G.S. and C.T. contributed new reagents/analytic tools; F.Z., B.K., R.M.F., M.Z., and X.L. analyzed data; and B.K., R.M.F., and X.L. wrote the paper.

The authors declare no conflict of interest.

*This Direct Submission article had a prearranged editor.

Freely available online through the PNAS open access option.

[1]To whom correspondence should be addressed. E-mail: xiaodong.li@senomyx.com.

This article contains supporting information online at www.pnas.org/cgi/content/full/0911660107/DCSupplemental.

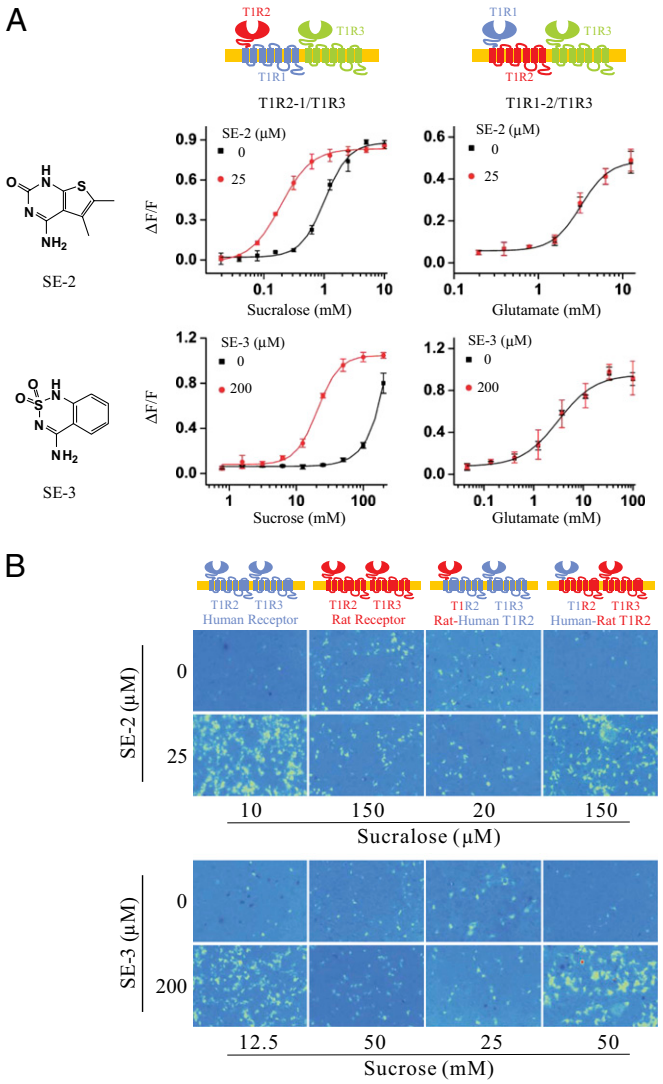

Fig. 1. Mapping of the sweet taste enhancer interaction site. (*A*) Sweet–umami chimeric receptors. hT1R2-1/hT1R3 and hT1R1-2/rT1R3 stable cell lines were assayed by using fluorescence imaging plate reader (FLIPR). Dose-dependent response curves of hT1R2-1/hT1R3 stable cell line were determined in the absence and presence of SE-2 for sucralose or SE-3 for sucrose. Dose–response curves of the hT1R1-2/hT1R3 stable cell line were determined in the absence and presence of SE-2 and SE-3 for glutamate. (*B*) Human–rat chimeric receptors. Human, rat, and two sets of human–rat chimeric T1R2 receptors were each cotransfected with either human or rat T1R3, as illustrated by the schematics on top, and assayed for SE-2 and SE-3 enhancement activities by using calcium imaging. The concentrations of sucralose and sucrose were different for different receptors, as shown. Those concentrations are approximately EC_{20} of their respective receptor.

T1R2 NED with the human counterpart made the receptor responsive to the enhancers. The results obtained using human-rat chimeric receptors confirmed the role of T1R2 NED in interaction with the SE-2 and SE-3.

Mutagenesis Studies. To further define the binding region for sweet taste enhancers, we carried out mutagenesis studies on the T1R2 VFT domain. Twenty-three residues within the T1R2 VFT domain were selected for mutagenesis based on sequence alignment with mGluRs and a molecular model of the T1R2 VFT domain (*Molecular Modeling*). Among the 23 mutants, 7 were found to have significantly reduced responses to sucralose or sucrose, whereas the enhancement activities of SE-2 and SE-3

Table 1. Summary of mutagenesis data

	Activities					
hT1R2	Sucralose	Sucrose	SE-2	SE-3	Stevioside	SWT819
WT	+	+	+	+	+	+
S40A	–	–	+	+	–	+
Y103A	–	–	+	+	–	+
D142A	–	–	+	+	–	+
P277A	+/–	+/–	+	+	+/–	+
D278A	–	–	+	+	+	+
E302A	–	–	+	+	–	+
R383A	–	–	+	+	–	+
K65A	+/–	+	–	–	–	+
L279A	+	+	–	–	+	+
D307A	+/–	–	–	–	–	+

Among the 23 T1R2 residues tested in the mutagenesis analysis, the 10 residues that are crucial for sucrose/sucralose and/or SE-2/SE-3 activities are listed. Wild-type and mutant T1Rs were each cotransfected with T1R3 and assayed by using either FLIPR or calcium imaging. Sucralose was used at 2.5 mM, sucrose at 100 mM, SE-2 at 25 μM in the presence of sucralose, and SE-3 at 200 μM in the presence of sucrose. Stevioside (0.6 mM) responses were determined to support the molecular model. SWT819 (25 μM) was used as a control for protein expression. The three residues required for enhancer activities are in the lowest three rows. +, comparable activity with the wild-type (WT) receptor; –, no detectable activity; +/–, reproducible activity significantly below that of wild-type receptor (see Figs. S1 and S2 for details).

were essentially not affected (Table 1 and Figs. S1 and S2). Y103A is a representative mutant of this class (Fig. 2*A*). When coexpressed with hT1R3, Y103A did not respond to sucralose up to 10 mM, >100 times higher than the EC_{50} for the wild-type receptor. Similarly, the mutant receptor did not respond to sucrose at 100 mM (Fig. 2*B*). SWT819 (12), a sweet receptor agonist that interacts with the T1R2 TM domain, was used as a control. Y103A did not affect SWT819 activity (Fig. 2*E*), indicating that the loss of sucralose and sucrose responses was not due to altered protein expression, misfolding, or poor membrane targeting. The enhancement activities of SE-2 and SE-3 were intact. The response to sucralose could be rescued by SE-2 (Fig. 2*A*) and that of sucrose by SE-3 (Fig. 2*B*).

Mutations of three residues affected the enhancement activities of SE-2 and SE-3. L279A is a typical example of this class of mutants. The dose–response curve of this mutant receptor to sucralose was identical in the presence or absence of 25 μM SE-2, which was sufficient to shift the EC_{50} of the wild-type receptor by 6-fold (Fig. 2*C*). Similarly, the response of L279A to sucrose was no longer potentiated by SE-3 (Fig. 2*D*). It should be noted that L279A also had a partial effect on the sucralose and sucrose activities (*Molecular Modeling*), shifting the dose–response curves to the right by about 5-fold, whereas the response to SWT819 was not changed (Fig. 2*E*).

Molecular Modeling. Homology models of the T1R2 VFT domain (Fig. 3 and Figs. S3 and S4) in open and closed forms were built using crystal structures of mGluR1, mGluR3, and mGluR7 (5, 6, 13) from the Protein Data Bank. Despite low overall sequence identity (~30%) of T1R2 to mGluR1, residues close to the hinge whose side chains point inward toward the active site show significant similarity (Fig. S5). The model showed similarities and differences both with mGluRs and with our previous model of T1R1.

The upper lobe of T1R2 has a large cavity that can explain the existence of a variety of large sweeteners that interact with the T1R2 VFT domain (Fig. 3*A*). In our model, sucrose and sucralose molecules interact with the backbone nitrogens of I167 and S144 and to the hydroxyl of S144 (Fig. 3*B* and Figs. S3 and S4). These residues are close to the hinge region of the VFT domain.

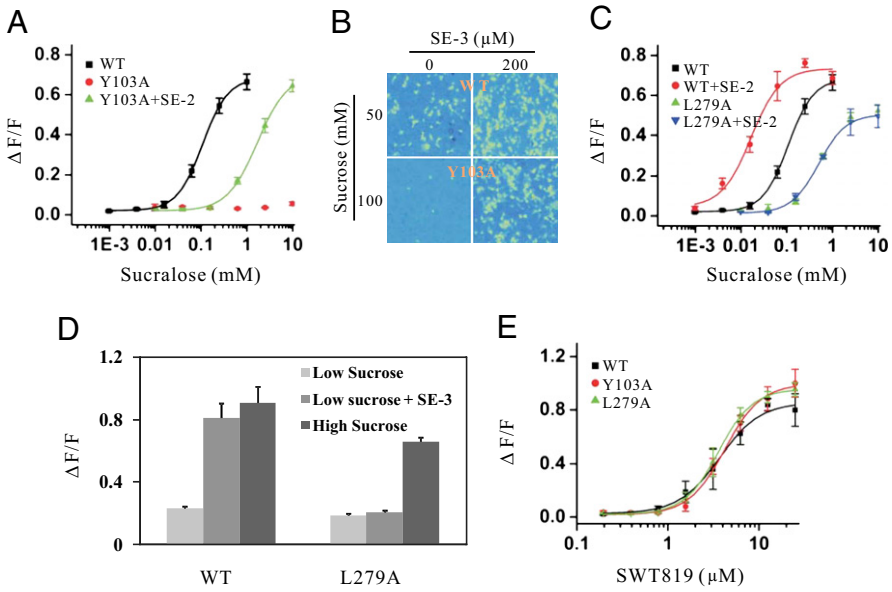

Fig. 2. Activities of T1R2 mutants Y103A and L279A. Human T1R2 mutants were each cotransfected with human T1R3 and assayed for sweetener and enhancer activities. The wild-type (WT) sweet taste receptor was used as a control. (*A*) Dose–response curves of T1R2(Y103A)/T1R3 for sucralose in the absence and presence of SE-2 (25 μM), determined by using FLIPR. (*B*) Responses of T1R2(Y103A)/T1R3 to sucrose in the absence and presence of SE-3, determined by using calcium imaging. (*C*) Dose–response curves of T1R2(L279A)/T1R3 for sucralose in the absence and presence of SE-2 (25 μM), determined by using FLIPR. (*D*) Responses of T1R2(L279A)/T1R3 to sucrose in the absence and presence of SE-3 determined by using FLIPR. Low sucrose = 50 mM for WT and 100 mM for L279A, high sucrose = 200 mM. (*E*) Dose–response curves of WT and the two mutant receptors for SWT819, determined by using FLIPR.

All hydroxyl groups of sucrose and sucralose made hydrogen bonds with adjacent hydrophilic residues such as D142 and E302, whereas the chlorines of sucralose found hydrophobic contacts with residues Y103 and P277. Similar active-site agonist binding residues were described in a previous article on T1R2 modeling with aspartame (14). The positioning of sucrose and sucralose follows the evolutionarily conserved mechanism of agonist–hinge interaction found in other VFT domains and is supported by site-directed mutagenesis. In particular, mutations of D142 and E302 to alanine abolished the activities of sucrose and sucralose. Mutation of S144 or I167 had no obvious effect, probably because of the interaction being mediated largely by the backbone nitrogens. The diminished responses of the seven mutants (S40, Y103, D142, D278, E302, P277, and R383) to sucralose and sucrose could all be rescued by SE-2 and SE-3, respectively, suggesting that these residues are not making direct contact with the enhancers and that the overall binding mode of the agonists in the presence of enhancers is not altered because of these mutations.

In our model, the newly discovered sweet taste enhancers bind adjacent to their agonists, with van der Walls and hydrogen bonding interactions possible between enhancers and sweeteners (Fig. 3 and Figs. S3 and S4). In the closed conformation with sucrose and SE-3, four residues (K65, L279, D278, and D307) surround and interact with the enhancer. Sucrose and SE-3 form direct contact through a hydrogen bond. K65 and D278 form direct electrostatic interactions. The ring nitrogen of bound SE-3 closest to K65 may be unprotonated (with a measured solution pK_a of 5.98), enhancing the compound's interaction with K65. The binding mode of sucralose/SE-2 follows a similar pattern (Fig. S4). Sucralose and SE-2 are in direct contact, and both form extensive hydrogen bonding patterns to residues in the active site. In our model, the two critical chlorines for SE-2 enhancement activity, 4-Cl and 6′-Cl, are not in direct contact with SE-2, but engage in hydrophobic interactions that may help orient the two rings of sucralose to more effectively interact with SE-2.

We introduced the term "pincer residues" to describe amino acids near the lips of the lobes involved in lobe-to-lobe interactions or lobe–enhancer interactions to help stabilize the closed conformation of the VFT domain. The extensive nature of interlobe connections in mGluRs was also noted previously (15). Direct interlobe interactions found in the closed conformation of mGluRs manifest as both electrostatic and hydrophobic interactions in the model of T1R2. Based on our model, the potential electrostatic pincer residues include R383 and K65 of the upper lobe and D278 and D307 of the lower lobe. The potential hydrophobic pincer residues include A43, V64, I67, Y103, and K65 of the upper lobe, and P277, L279, and V309 of the lower lobe. K65 appears to be involved in both electrostatic and hydrophobic interactions. In our model, these residues located on the opposite lobes do not contact each other in the open conformation but are positioned to interact upon lobe closure (Fig. 4*B*). It is worth noting that the hydrophobic pincer interaction was absent in our umami receptor model. The role of K65 and D278 as electrostatic pincer residues was supported by the activities of the D278K/K65D double mutant (see details in the next section). Even though these residues are not in direct contact with sucrose or sucralose in our model, mutations of some of these residues (K65, Y103, L279, D307, and R383) still resulted in a diminished response to the sweeteners (Figs. S1 and S2). This is probably due to the critical role of these residues in stabilizing the closed conformation.

We hypothesize that the activation of the T1R2 VFT domain follows a two-step mechanism as proposed in the case of mGluRs: attachment of ligands to the upper lobe (docking) followed by lobe closure (locking) (16–18). Based on the dynamics of the closure of the iGluR2 VFT domain, the two steps proceed on two different time scales—i.e., approximately microseconds for docking and approximately milliseconds for locking. Consequently, in this dynamic model the opening between the lobes is exposed for a long (approximately milliseconds) time frame, making cooperative attachment of both sweeteners and modulators to the upper lobe possible. The dif-

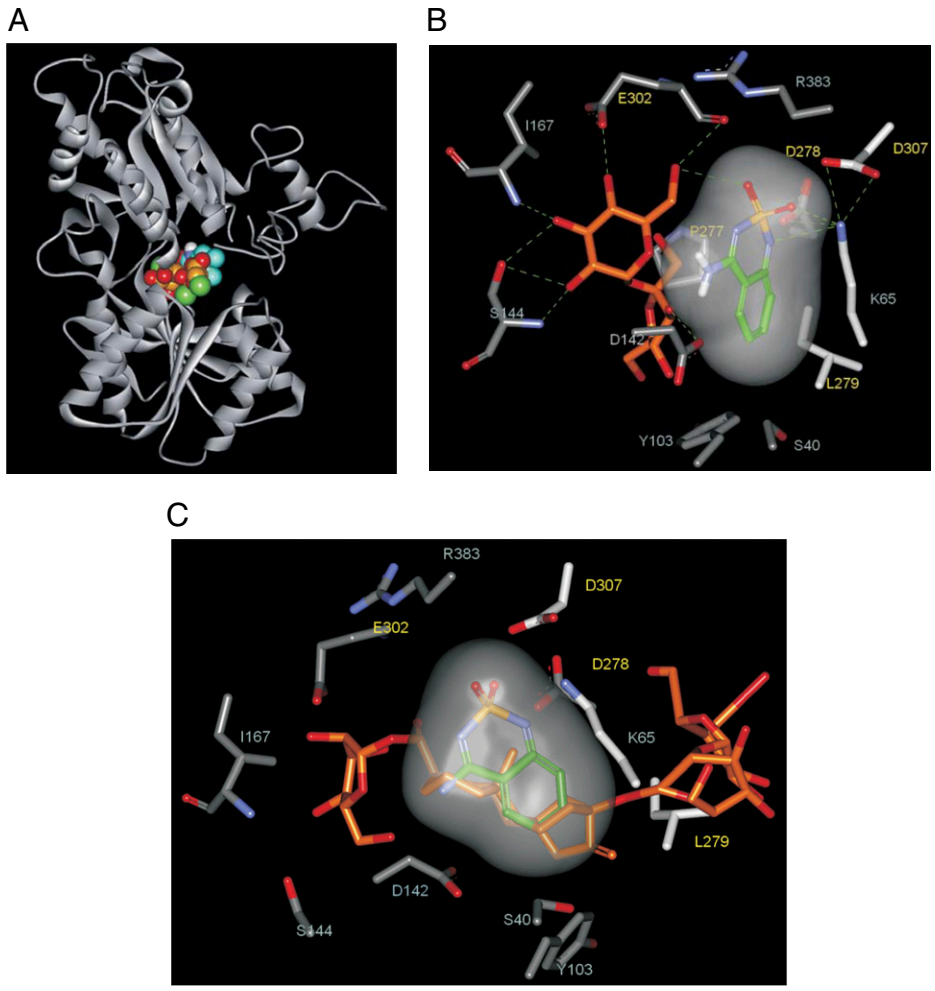

Fig. 3. A molecular model of the T1R2 VFT domain. (*A*) The T1R2 VFT domain in a closed conformation with bound sucralose (carbon atoms in gold, oxygen in red, and chlorine in green) and SE-2 (carbon atoms in cyan). Sucralose and SE-2 are adjacent to each other between the two lobes of the flytrap. (*B*) A close view of the ligand binding pocket looking down from above the upper lobe with sucrose and SE-3 bound. Lower lobe residues are labeled in yellow letters and upper lobe residues in gray letters. Sucrose is in gold; SE-3 is in green and is encased in a gray surface. The three residues critical for enhancer activities (K65, L279, and D307) are in white, and the seven residues critical for sucrose/sucralose activities (S40, Y103, D142, D278, E302, P277, and R383) are in gray. (*C*) A model of the binding pocket with bound stevioside [shown in a slightly different angle from *B* to allow a better view of the stevioside molecule]. Carbon atoms of stevioside are in orange. A molecule of the SE-3 enhancer is also shown in this model to illustrate the overlapping positioning of the enhancer and the steviol backbone. The carbon atoms of the enhancer are in green, and the molecule is shown with a surrounding gray surface. The single glucose moiety of stevioside is positioned to overlap with the sucrose in *B*.

ference in the timing of docking and locking reflects the existence of an entropic penalty that must be compensated by enthalpic free energy contributions during lobe closure. The free energy entropic penalties come from (*i*) restriction of backbone motions of the hinge through interaction with the sweeteners, (*ii*) restriction of side chain motions of contact residues to sweeteners and enhancers, and (*iii*) restriction of relative lobe movement due to sweetener and enhancer binding.

Many large sweeteners, with much higher affinity than sucrose for the sweet taste receptor, interact with the T1R2 VFT domain (unpublished data). A main conjecture of our model is that the newly discovered sweet taste enhancers share the same binding pocket as those of large sweeteners, such as stevioside, superaspartame, and SC-45647.

We used stevioside as an example to illustrate the point (Fig. 3*C*). In our model, the sucrose–enhancer complexes spatially overlap with stevioside and fit in the same upper lobe cavities. The single glucose moiety of stevioside is positioned to occupy the same space as sucrose/sucralose, whereas the steviol backbone overlaps with the sweet enhancer molecules. The double glucose moiety extends out of the VFT domain. The combined effect of sucrose/sucralose and enhancers results in a binding mode that mimics the binding mode of stevioside. The model of stevioside binding is supported by the mutagenesis data. The critical residues in Table 1 can be divided into two groups, with one group located near the hinge region adjacent to sucrose/sucralose and the other located close to the enhancers. The majority of the residues from both groups are required for stevioside activity (Table 1). One notable exception is the L279A mutation that does not affect stevioside. This can be explained by the size of stevioside, which already makes extensive hydrophobic interactions within the active site. A small reduction in hydrophobic interactions will not noticeably affect the binding free energy.

Electrostatic Interaction Between K65 and D278. D278 is one of the pincer residues required to stabilize the closed conformation of the T1R2 VFT domain. D278A had no detectable response to sucralose or sucrose, but the responses could be rescued by low concentrations of SE-2 and SE-3, respectively (Figs. S1 and S2).

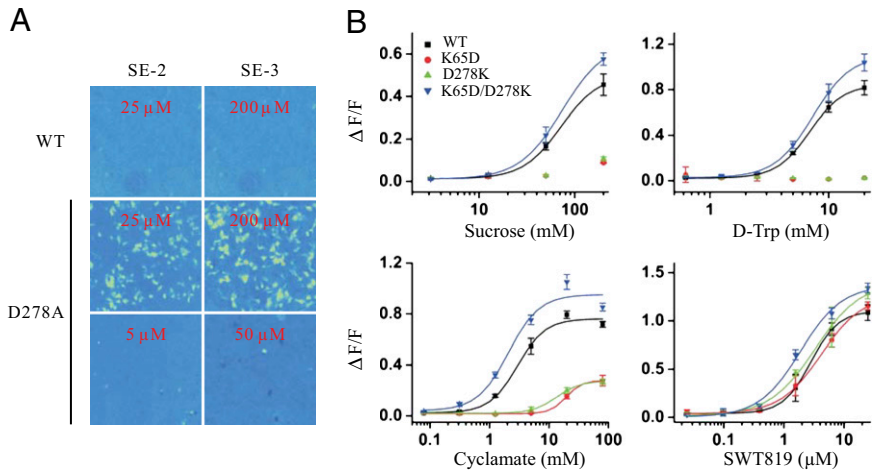

Fig. 4. Mutagenesis of electrostatic pincer residues K65 and D278. (*A*) T1R2 wild-type (WT) and mutant (D278A) were cotransfected with T1R3 and assayed by using calcium imaging for SE-2 and SE-3. (*B*) WT human T1R2, K65D, and D278K single mutants, and K65D/D278K double mutant were each cotransfected with T1R3 and assayed using FLIPR. Dose–response curves for sucrose, D-tryptophan, cyclamate, and SWT819 were determined for the four receptors.

Surprisingly, SE-2 and SE-3 elicited straight agonist responses on D278A at higher concentrations in the absence of sucralose or sucrose (Fig. 4*A*). No response was observed on the wild-type receptor at the same concentration of SE-2 and SE-3. We speculate that the D278A mutant may provide additional hydrophobic contact between the enhancers and lower lobe, enabling the enhancers to activate the receptor without the sweeteners.

The model suggests that D278 stabilizes the closed conformation of the T1R2 VFT domain through interaction with K65 on the opposite lobe. To test this hypothesis, we generated mutants that reverse the charges of D278 and K65, individually and in combination (K65D, D278K, and K65D/D278K double mutant; Fig. 4*B*). Reversing the charge on either K65 or D278 individually abolished the response of the receptor to sweeteners including sucrose, D-tryptophan, and even cyclamate. However, the responses to those sweeteners were rescued by the double mutant, indicating that the opposite charges of the pincer residues on the two lobes are important for the receptor activity. This observation argues that the electrostatic interactions between K65 and D278 are critical for the sweet taste receptor activities, providing strong support for our hypothesis that these two residues form a salt bridge upon the closure of the T1R2 VFT domain to stabilize the active conformation. It is somewhat surprising to us that even cyclamate required the opposite charges of the opposite pincer residues, because this is a sweetener that interacts with the TM domain of T1R3. It is likely that activation of the sweet taste receptor by cyclamate still requires conformational changes in the T1R2 VFT domain. In contrast, SWT819 probably activates the receptor through a different mechanism, as the compound can activate all three charge reversing mutants.

In summary, our data generated using chimeric T1R receptors indicate that the two sweet taste enhancers interact with the VFT domain of T1R2. Results from molecular modeling and mutagenesis studies strongly argue that the sweet taste enhancers follow a similar mechanism to that of the umami taste enhancers IMP and GMP. Sweeteners bind near the hinge region and induce initial closure of the VFT domain, whereas the enhancer molecules bind near the opening of the pocket and further stabilize the closed conformation by strengthening the hydrophobic interactions between the two lobes and lowering the entropic penalties of lobe closure. Through cooperative binding with agonists in the VFT domains, this group of positive allosteric modulators for T1R taste receptors represents a unique mechanism of class C GPCR modulation.

Materials and Methods

Stable Cell Lines. As previously described, hT1R2-1/hT1R3 stable cell lines were generated by transfecting linearized pCDNA3.1/Neo-derived T1R2-T1R1 and pCDNA3.1/Zeo-derived (Invitrogen) T1R3 vectors into a $G_{16gust25}$ cell line, an HEK 293 line stably expressing the chimeric $G_{16gust25}$ protein. Cells were selected with 0.4 mg/mL G418 (Invitrogen) and 0.1 mg/mL zeocin (Invitrogen) in low-glucose DMEM. hT1R1-2/rT1R3 stable cell lines were generated by transfecting linearized pEAK10-derived T1R1-T1R2 and pCDNA3.1/Zeo-derived (Invitrogen) T1R3 vectors into a $G_{16gust44}$ cell line, an HEK 293 line stably expressing the chimeric $G_{16gust44}$ protein (19). Cells were selected with 0.5 μg/mL puromycin (Calbiochem) and 50 μg/mL zeocin (Invitrogen) in glutamine-free DMEM supplemented with GlutaMAX. Resistant colonies were expanded, and their responses to sweet and umami taste stimuli were evaluated by calcium imaging.

Chimeric Receptors. As previously described, T1R chimeras were constructed by introducing an XhoI site with a silent mutation at human T1R2 amino acid 560. T1R mutants were generated by using a standard PCR-based mutagenesis protocol. All T1Rs, chimeras and mutants used in the HEK 293 cell-based assay were cloned into the pEAK10 expression vector (EdgeBio).

HEK Cell-Based Assay. The calcium imaging assay was performed as described in refs. 1 and 12. Assays using a fluorescence imaging plate reader (FLIPR) were performed using 384-well plates (~20,000 cells per well). Transient transfections were performed in suspension using Mirus *Trans*It-293 (Invitrogen). Briefly, ~10^7 cells were mixed with 20 μg of DNA lipid complex, incubated at room temperature for 20 min, and seeded onto 384-well plates.

Mutagenesis Studies. Mutagenesis was performed by using a standard PCR-based method. The following 23 residues in human T1R2 (GenBank entry BK000153) were mutated individually to Ala: S40, K65, I67, Y103, D142, N143, S144, S165, I167, T184, Y215A, T242, P277, D278, L279, E302, S303, D307, T326, Q328, E382, R383, and V384. Each T1R2 mutant was transiently cotransfected with human T1R3 into the $G_{16gust25}$ cell and assayed using FLIPR or calcium imaging.

Molecular Modeling. Homology models of the T1R2 VFT domain were constructed with the program Homology (Accelrys) by using available structures from the Protein Data Bank: 1EWK, 1EWT, 1EWV, and 3KS9 of the metabotropic glutamate receptors mGluR1; 2E4U, 2E4V, 2E4W, 2E4X, and 2E4Y of mGluR3; and 2E4Z of mGluR7. Ligands were introduced into the model by using the program Biodock (BioPredict). Resulting complexes were subjected to minimization and molecular dynamics-based simulated

annealing both with and without explicit water molecules by using the program Gromacs (www.gromacs.org). Normal modes were computed by also using Gromacs.

ACKNOWLEDGMENTS. We thank J. Kang for his scientific contribution in molecular modeling, and B. Moyer, A. Pronin, and D. Linemeyer for critical reading of the manuscript.

1. Li X, et al. (2002) Human receptors for sweet and umami taste. *Proc Natl Acad Sci USA* 99:4692–4696.
2. Nelson G, et al. (2002) An amino-acid taste receptor. *Nature* 416:199–202.
3. Nelson G, et al. (2001) Mammalian sweet taste receptors. *Cell* 106:381–390.
4. Pin JP, Galvez T, Prézeau L (2003) Evolution, structure, and activation mechanism of family 3/C G-protein-coupled receptors. *Pharmacol Ther* 98:325–354.
5. Kunishima N, et al. (2000) Structural basis of glutamate recognition by a dimeric metabotropic glutamate receptor. *Nature* 407:971–977.
6. Muto T, Tsuchiya D, Morikawa K, Jingami H (2007) Structures of the extracellular regions of the group II/III metabotropic glutamate receptors. *Proc Natl Acad Sci USA* 104:3759–3764.
7. Schiffman SS, Booth BJ, Losee ML, Pecore SD, Warwick ZS (1995) Bitterness of sweeteners as a function of concentration. *Brain Res Bull* 36:505–513.
8. Schiffman SS, Gatlin CA (1993) Sweeteners: state of knowledge review. *Neurosci Biobehav Rev* 17:313–345.
9. Yamaguchi S, Ninomiya K (2000) Umami and food palatability. *J Nutr* 130 (4S,suppl): 921S–926S.
10. Zhang F, et al. (2008) Molecular mechanism for the umami taste synergism. *Proc Natl Acad Sci USA* 105:20930–20934.
11. Conn PJ, Christopoulos A, Lindsley CW (2009) Allosteric modulators of GPCRs: a novel approach for the treatment of CNS disorders. *Nat Rev Drug Discov* 8:41–54.
12. Xu H, et al. (2004) Different functional roles of T1R subunits in the heteromeric taste receptors. *Proc Natl Acad Sci USA* 101:14258–14263.
13. Tsuchiya D, Kunishima N, Kamiya N, Jingami H, Morikawa K (2002) Structural views of the ligand-binding cores of a metabotropic glutamate receptor complexed with an antagonist and both glutamate and Gd3+. *Proc Natl Acad Sci USA* 99:2660–2665.
14. Cui M, et al. (2006) The heterodimeric sweet taste receptor has multiple potential ligand binding sites. *Curr Pharm Des* 12:4591–4600.
15. Bertrand HO, Bessis AS, Pin JP, Acher FC (2002) Common and selective molecular determinants involved in metabotopic glutamate receptor agonist activity. *J Med Chem* 45:3171–3183.
16. Abele R, Keinanen K, Madden DR (2000) Agonist-induced isomerization in a glutamate receptor ligand-binding domain. A kinetic and mutagenetic analysis. *J Biol Chem* 275:21355–21363.
17. Ahmed AH, Loh AP, Jane DE, Oswald RE (2007) Dynamics of the S1S2 glutamate binding domain of GluR2 measured using 19F NMR spectroscopy. *J Biol Chem* 282: 12773–12784.
18. Lau AY, Roux B (2007) The free energy landscapes governing conformational changes in a glutamate receptor ligand-binding domain. *Structure* 15:1203–1214.
19. Ueda T, Ugawa S, Yamamura H, Imaizumi Y, Shimada S (2003) Functional interaction between T2R taste receptors and G-protein alpha subunits expressed in taste receptor cells. *J Neurosci* 23:7376–7380.